

# Thesis Title

*A subtitle of your thesis*

Author name



Thesis submitted for the degree of  
Master in Master's Program Name <change at  
main.tex>  
60 credits

Department Name <change at main.tex>  
Faculty name <change in duoforside.tex>

UNIVERSITY OF OSLO

Spring 2022



# Thesis Title

*A subtitle of your thesis*

Author name

© 2022 Author name

Thesis Title

<http://www.duo.uio.no/>

Printed: Reprosentralen, University of Oslo

# **Abstract**

# Contents

<b>1</b>	<b>Introduction</b>	<b>1</b>
<b>I</b>	<b>Theory</b>	<b>3</b>
<b>2</b>	<b>Background</b>	<b>4</b>
2.1	Overview of sold-state physics . . . . .	4
2.2	3d Silicides . . . . .	4
<b>3</b>	<b>High-Entropy alloys</b>	<b>5</b>
3.1	Fundamentals . . . . .	5
3.2	Core effects and properties of high-entropy alloys . . . . .	8
<b>4</b>	<b>Special quasi-random Structures</b>	<b>10</b>
4.1	The fundamentals of SQS . . . . .	10
4.2	Mathematical formulation . . . . .	11
4.3	Application of SQS to high-entropy alloys - Add figure . . . . .	13
<b>5</b>	<b>Density-Functional Theory</b>	<b>15</b>
5.1	Review of Quantum Mechanics . . . . .	15
5.1.1	The Shrödinger equation . . . . .	15
5.1.2	Simplifications and approximations to solve the many-electron Shrödinger equation . . . . .	16
5.2	Fundamentals of Density-Functional Theory . . . . .	17
5.3	Limitations of DFT . . . . .	18
<b>II</b>	<b>Methodology and Implementation</b>	<b>20</b>
<b>6</b>	<b>Practical application of DFT</b>	<b>21</b>
6.1	The Exchange-Correlation functional . . . . .	21
6.2	Fundamental aspects of practical DFT calculations . . . . .	22
6.3	Self-consistent field calculation . . . . .	24
<b>7</b>	<b>Computational details</b>	<b>26</b>
7.1	Vienna Ab initio Simulation Package . . . . .	26
7.2	Generation of SQS . . . . .	28
7.3	Band-structure . . . . .	28

7.4 Utility scripts . . . . .	30
<b>III Results and Discussion</b>	<b>32</b>
8 Working title	33
<b>IV Conclusion</b>	<b>46</b>

# List of Figures

3.1	Formation of HEA based on $\delta$ and $N$ . Figures adopted from [hea2016_ch2] . . . . .	7
3.2	A schematic illustration of lattice distortion in high-entropy alloys. Figure from [owen_jones_2018] . . . . .	9
6.1	Self consistent iteration of a DFT calculation. Figure adopted from lecture notes fys-mena4111 cite . . . . .	25
7.1	48 atom SQS based on eqvimolar distribution of Cr, Fe, Mn and Ni in and $FeSi_2$ cell. . . . .	29
8.2	Density of states for structure A, B, C, D, E of CFMNSi <sub>2</sub> ( $FeSi_2$ ) SQSs (PBE GGA) . . . . .	36
8.3	Band gap of CFMN fesi2 SQSs in spin up and spin down with PBE functional. . . . .	38
8.5	E . . . . .	40
8.9	Band gap of CFMN (fesi2) all 5 SQSs with PBE, SCAN and HSE06 . . . . .	44
8.10	Density of states from HSE06 of $FeSi_2$ CFMN structure B . . .	44
8.11	The density of states of CFMN ( $FeSi_2$ ) structure E for a) spin up and down, and b) focused on spin down . . . . .	45



# List of Tables

- 8.1 Total energy per atom, final magnetic moment, and band gap  
(GGA) of 5  $Cr_4Fe_4Mn_4Ni_4Si_{32}$  SQSs based on  $FeSi_2$  . . . . . 34
- 8.2 Band gap transition of CFMN (fesi2) SQSs with PBE functional 34

# Preface

# Chapter 1

## Introduction

some introduction on the importance of discovering new materials and alloying.

High-entropy alloys is a novel class of materials based on alloying multiple components, as opposed to the more traditional binary alloys. This results in an unprecedented opportunity for discovery of new materials with a superior degree of tuning for specific properties and applications. Recent research on high-entropy alloys have resulted in materials with exceedingly strong mechanical properties such as strength, corrosion and temperature resistance, etc **find references**. Meanwhile, the functional properties of high-entropy alloys is vastly unexplored. In this study, we attempt to broaden the knowledge of this field, the precise formulation of this thesis would be an exploration on the possibilities of semiconducting high-entropy alloys.

A key motivation of this thesis is the ability to perform such a broad study of complex materials in light of the advances in material informatics and computational methods. In this project, we will employ Ab initio methods backed by density functional theory on top-of the line supercomputers and software. 20 years ago, at the breaking point of these methods, this study would have been significantly narrower and less detailed firstly, but secondly would have totaled ... amount of CPU hours to complete (**Calculate this number**). In the addition to the development in computational power, is also the progress of modeling materials, specifically we will apply a method called Special Quasi-random Structures (SQS) to model high-entropy alloys or generally computationally complex structures. Together with the open landscape of high-entropy alloys described above, these factors produce a relevant study in the direction of applying modern computational methods to progress the research of a novel material class and point to promising directions for future research.

In specifics, this thesis revolve around the electrical properties of high-entropy alloys, mainly the band gap as this is the key indicator for a semiconducting material and it's applicability. Semiconductors are the building blocks in many different applications in today's world, ranging from optical and electrical devices, to renewable energy sources such as

solar and thermoelectricity. Given the economic and sustainable factors concerning silicon, in addition to its role in relevant applications such as microelectronics and solar power. Silicon emerges as a natural selection to build our alloys around. Furthermore, the development and research on both high entropy alloys and metal silicides have been heavily centered around 3d transition metals. Keeping in line with the economic and environmental factors, we will continue this direction by focusing on high entropy stabilized sustainable and economic 3d metal silicides **Not happy with this writing**. Throughout the study we will analyze a great number of permutations of 3d silicides, from different initial metal silicides such as  $CrSi_2$ ,  $FeSi_2$ ,  $MnSi_{1.75}$ ,  $Fe_2Si$ , each with distinct properties relating to the band gap, crystal structure and metal to silicon ratio. In addition, the permutations include numerous metal distributions and elements within the 3d-group of metals. Examples are Co, Cr, Fe, Mn, and Ni.

Given a background in high-entropy alloys, one could ask if this study is truly sensible. In the later sections we will cover the details of this field, and it quickly become clear that the materials investigated in this study does not fall under the precise definition of high-entropy alloys, nor do we intend to explore the properties and factors relating to high-entropy stabilized alloys such as the configurational entropy, phase stability and finite temperature studies. However this study is motivated from the discovery of these materials and promising properties, and venture into a more hypothetical space of materials, enabled by the computational methods available to study the potential properties of such materials. On the other hand, very recent studies **Mari, and other HEA silicide study** have experimentally produced high-entropy disilicides, thus in some way justifying the direction of this project.

We begin this project by reviewing key concepts of solid-state physics for readers lacking a background in materials science, and an introduction to the base 3d silicides of the experimental work. Later follows a theoretic walk-through of the relevant concepts of this thesis, these topics include high-entropy alloys, special quasi-random structures, and density functional theory. Next we shine light on the implementation of DFT in this project, and other computational details required to reproduce the results in this thesis, such as the use of the Vienna Ab Initio Simulation Package (VASP) and implementation of SQS. Finally we present the results of our study, these include the band gap and electronic properties of various structures and the success and challenges of the computational methods applied throughout the study.

# **Part I**

# **Theory**

## **Part II**

# **Methodology and Implementation**

mm

**Part III**

**Results and Discussion**



## Chapter 8

# Working title

Throughout the duration of this study, we have carried out a great number of DFT calculations in order to present an comprehensive overview of promising high-entropy silicides. In payment to the thermoelectric prospect of hexagonal  $Fe_2Si$ , we firstly attempted to build SQSs from this structure. However, in agreement to the experimental indication that **cite?**, 3d silicides adopt a metallic character when the 3d elements supercede 50% of the composition, all of our SQSs displayed a clear absence of an energy gap between the valence band and conduction band, we will return more specifically to these compositions later in this section. For now, we will present the results of a much more interesting and promising case, in which we replaced  $Fe_2Si$ , with  $\beta - FeSi_2$ , effectively doubling the Si-metal ratio. Hence why we prefer the term high-entropy silicides more so than high-entropy alloys, as these particular compositions does not lie directly within the conditions presented in sections (**HEA**). In this structure, we completed in total calculations regarding 17 distinct compositions and permutations, such ALLOYSi<sub>2</sub> SQS based on CoCrFeni, CrFeMnNi, CoCrMnNi, CrFeMnTi, CrFeTiNi, and permutations within these such as increasing or decreasing the distribution of certain elements. Of the 17 variants, each consists of 5 unique SQSs, and trialed with numerous functionals, magnetic configurations and other parameters, as discussed in section .., in attempt to locate the overall most stable and reliable results. With this approach, the complete number of calculations and results both escalated very quickly, therefore, in the intent of presenting a clear and informative report of the study, we will begin this section by analyzing the overall most promising structure, then present and discuss these results in relation to the remaining permutations and structures.

The aforementioned system is composed of Cr, Fe, Mn, and Ni, equally distributed in a 48 atom SQSs of  $FeSi_2$ , whereas 32 of these is silicon atoms. Here after, this system will be abbreviated CFMN (fesi2) to specify that its within the framework of the cmce  $FeSi_2$  unit cell.

The 5 distinct SQS can be seen in figure (method/SQS). Bellow, in table ?? we present a summary of the total energy, final magnetic moment and band gap corresponding to the 5 SQSs called A, B, C, D, and E respectfully. From a first glance, we observe very similar properties between the

structures. The total energy per atom vary by 0.0092 eV from the most stable structure C ( $-6.6063$  eV) to the least stable structure D ( $-6.6155$  eV). Similarly, the final magnetic moment is near identical throughout the span of SQSs, which is excepted given that aside from the unique distribution, all 5 SQSs contain the same amount and type of elements. On the contrary to the magnetic moment, the band gap is very sensitive to the type of SQS, ranging from a highest 0.05 eV in structure B to 0, ie nonexistent in structure D. A band gap in this range means for excellent application as thermoelectric materials.

Structure	Total energy/atom (eV)	Final magnetic moment (?)	Band gap (eV)
<b>A</b>	-6,6080	4.0006	0.0280
<b>B</b>	-6,6138	3.9999	0.0523
<b>C</b>	-6,6063	4.0008	0.0344
<b>D</b>	-6,6155	4.0001	0
<b>E</b>	-6,6089	4.0000	0.0495

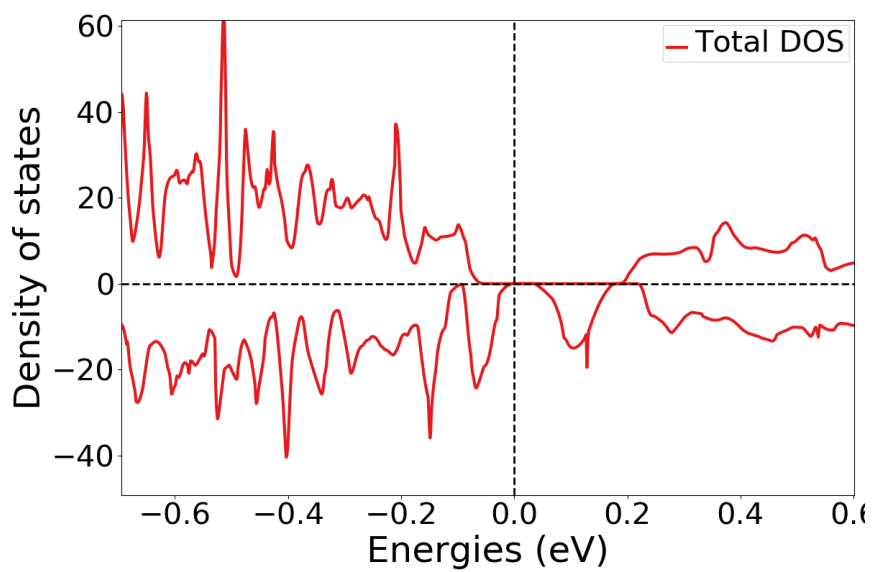
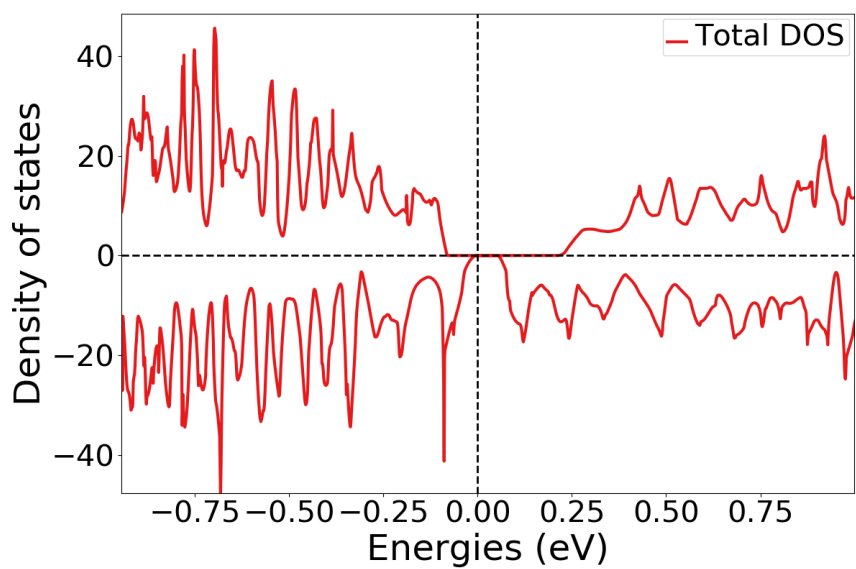
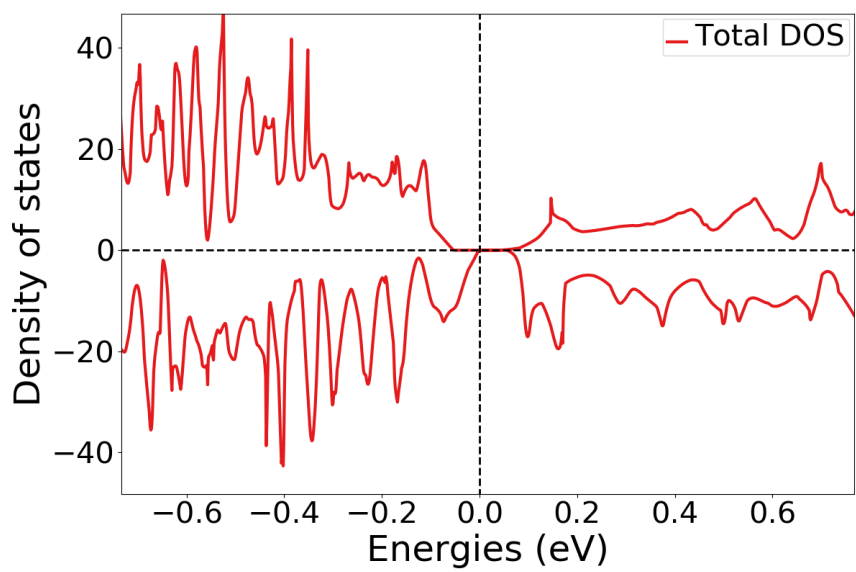
Table 8.1: Total energy per atom, final magnetic moment, and band gap (GGA) of 5  $Cr_4Fe_4Mn_4Ni_4Si_{32}$  SQSs based on  $FeSi_2$

Furthermore regarding the band gaps, we note that the gaps are indirect, the specific transitions is listed bellow.

Structure	Gap (D/I)	Transition
<b>A</b>	I	(0.500,0.333,0.500)-(0.500,0.000,0.000)
<b>B</b>	I	(0.250,0.000,0.250)-(0.000,0.000,0.000)
<b>C</b>	-	(0.500,0.000,0.500)-(-0.250,0.333,0.500)
<b>D</b>	I	-
<b>E</b>	I	(0.000,0.000,0.000)-(0.250,0.000,0.250)

Table 8.2: Band gap transition of CFMN (fesi2) SQSs with PBE functional

In this regard, it would have been very instructive to plot a band structure diagram to further evaluate the energy bands, however due to the complex nature of the SQSs and the implementation with TDEP we were not able to plot the bandstructure. Thus, in this section we will analyze the band gap by other meassures. The first method we will employ is to observe the band gap from the plotted density of states, in figure **ref bellow**. From these figures, we can determine the band gap from the distance in energy around the Fermi energy (here set to 0), where the density of states is exactly 0, in addition we can observe the band gap for spin  $\uparrow$  (positive) and  $\downarrow$  (negative) states.



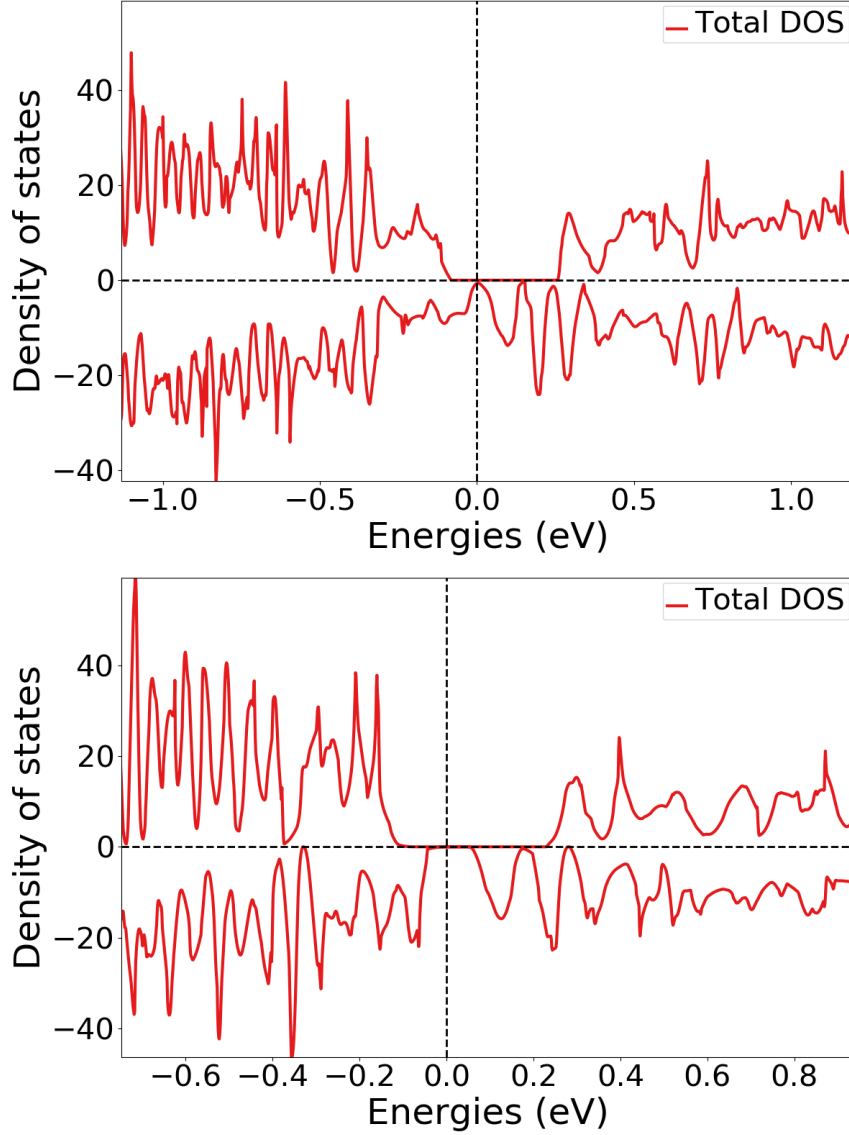


Figure 8.2: Density of states for structure A, B, C, D, E of  $CFMNSi_2(FeSi_2)$  SQSs (PBE GGA)

The most obvious result of figure (ref DOS above), is that the band gap listed for the five structures in table is validated from the density of states. The band gap for a spin-polarized system can be determined by the minimum distance between occupied states regardless of spin states. Thus, despite clear gap in the spin up direction, the total gap is often limited to the smaller or non-existent gap in the spin down channel. This is particularly evident in structure D, where there exist a large symmetric gap in spin  $\uparrow$  around 0.3 eV, but the metallic spin down channel results in an overall metallic band structure, as opposed to the remaining structures. Especially structures B and E show large gaps around 0.5 eV.

However, judging the band gap of a system solely based on the density of states, particularly in VASP, provide both limited information and are

prone to errors. For instance, all though the DOS illustrate that structure D have a gap in the  $\uparrow$  direction, but not in  $\downarrow$ , it does not provide an answer to why this is. Additionally, the accuracy of of the DOS is very sensitive to primarily the type of numerical smearing. In this project we observed a great number of cases where the density of states failed to capture the band gap when we employed Gaussian smearing, compared to the much more accurate method of tetrahedron smearing with Bloch corrections (see section method..) As well other computational factors such as number of points used to plot the DOS (NEDOS in VASP) and amount of k-points (to solve the DOS integral, see section ..).

A more rigid approach to both determine and investigate the band gap and structure of a solid with VASP and DFT is to investigate the Kohn-Sham eigenvalues. The eigenvalues are given for all energy bands for the given number of k-points used in the calculation, with listed energies and corresponding occupancy in both channels. In this structure, we find good agreement between the DOS and eigenvalues for the CFMN (fesi2) system. In figure **ref bar graph spin up/down** we illustrate the relationship between the spin up and down channels in regards to the band gap, as read from the eigenvalues. From the eigenvalues, we can qualitatively differentiate structure D from the rest, by observing that for certain k-points, the occupancy does not transition from 1 to 0 in 1 step, but rather contain partially occupied states in between, however only in the spin down channel. If we were to neglect this partially occupied states, and only consider bands with above 0.99 or bellow 0.01 occupancy, the band gap of structure D remain consistent in spin up, but we now observe a band gap in spin down around 0.05 eV and similarly thus for the total band gap of the structure. **More on this, and/or make some kind of figure to better explain it** Again, this would have been extremely insightful to investigate from the band structure of the structure.

Regarding the eigenvalues, there are some important factors to consider that may negatively impact the results. Firstly, as explained above the eigenvalues of each band is given for the total number of k-points employed in the calculation, obviously this leads to a relationship between accuracy and number of points. A small mesh of k-points may lead to the smallest transition between the highest occupied state in the conduction band and the lowest unoccupied state in the valence band risk not being encapsulated, resulting in an inaccurately large gap. As well, the eigenvalues are subject to the smearing method similarly, but inversely to the density of states. In this case, the tetrahedron method with Bloch corrections are prone to yield nonphysical results with the occupancy in a given band either above 1 or negative, ie bellow 0, whereas Gaussian smearing with an appropriately small smearing width. Due to the limited time and resources on this project, we were not able to investigate this principle to the full extent, and thus the listed results comes with a degree of uncertainty. An interesting observation in this project, is that out of all the numerous structures we studied, this problem of non-physical eigenvalues only appear in structures that does not have a band gap, and correspondingly contain these partial occupants. **More on this**

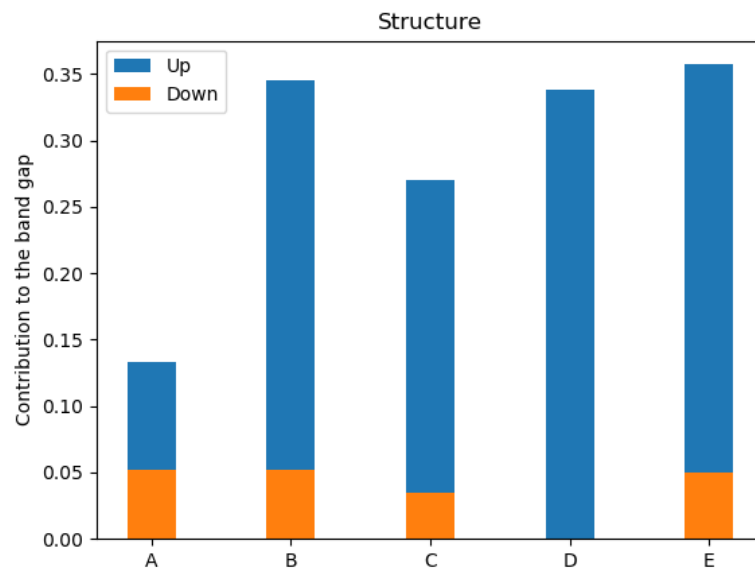
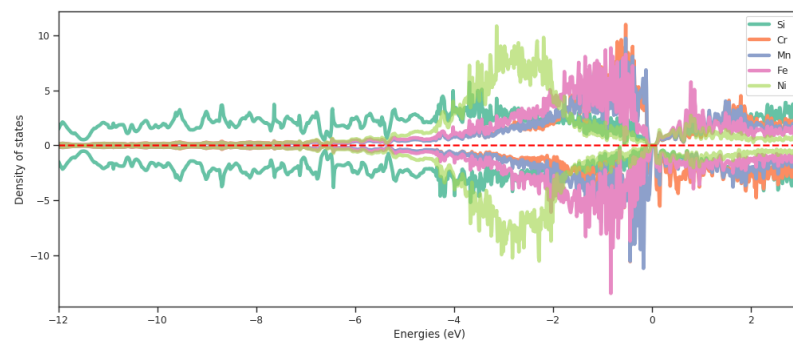


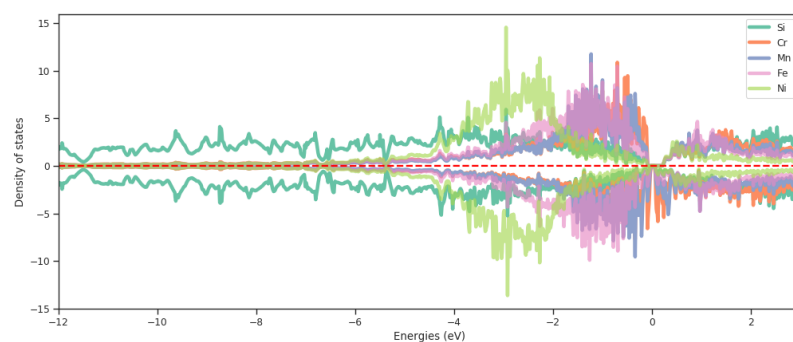
Figure 8.3: Band gap of CFMN fesi2 SQSs in spin up and spin down with PBE functional.

**Intro LDOS**

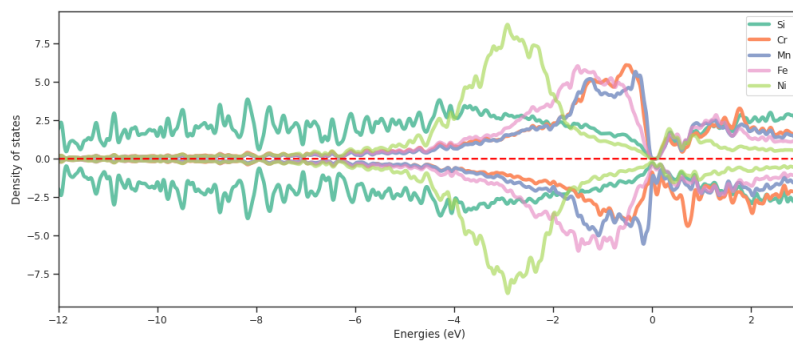
**Diskusjon LDOS**



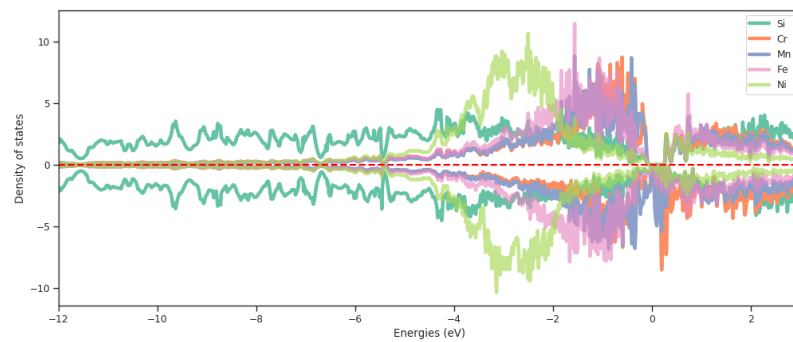
(a) A



(b) B



(c) C



(d) D

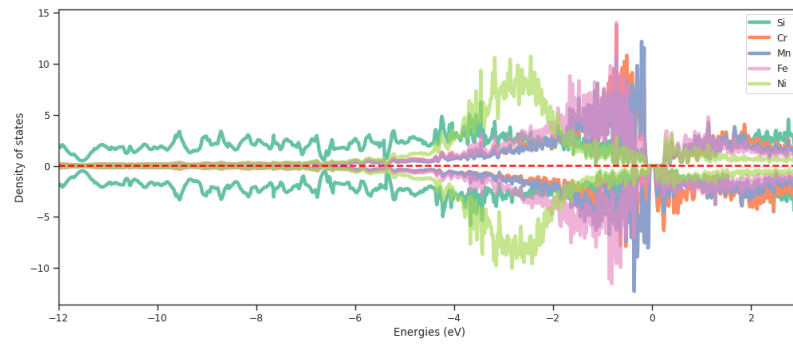
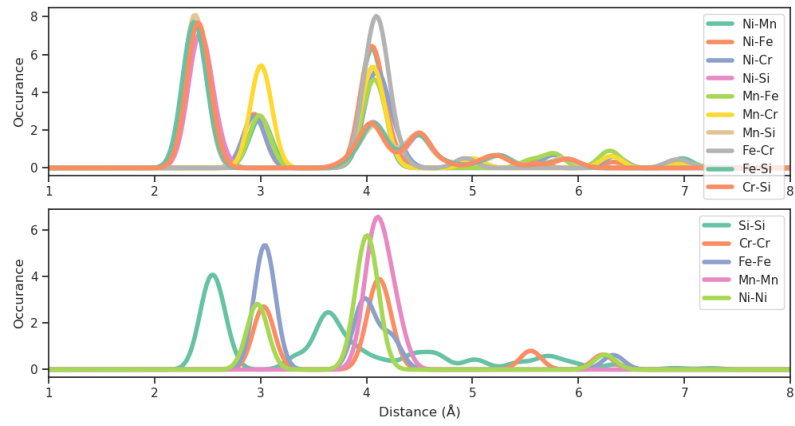


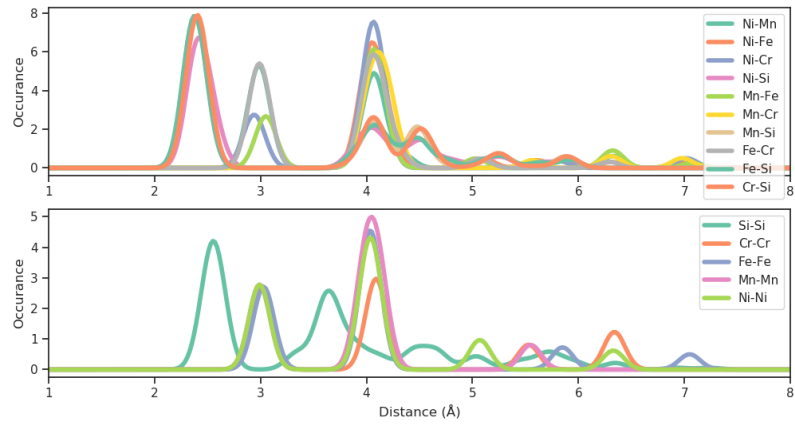
Figure 8.5: E

**Continue discussion LDOS, introduce and discuss PDFs**

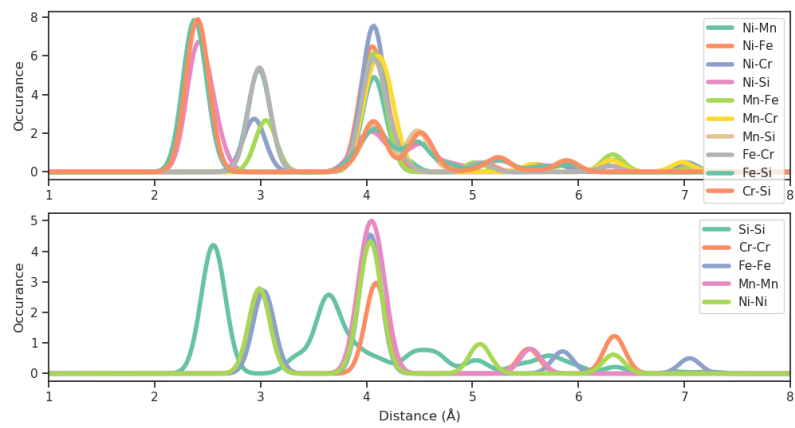




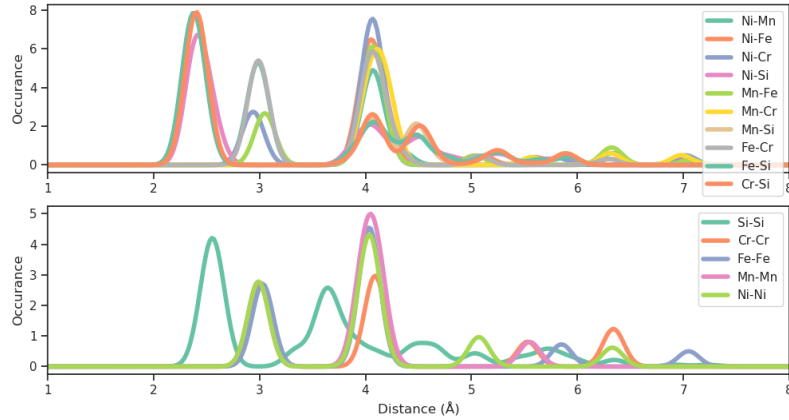
(a) A



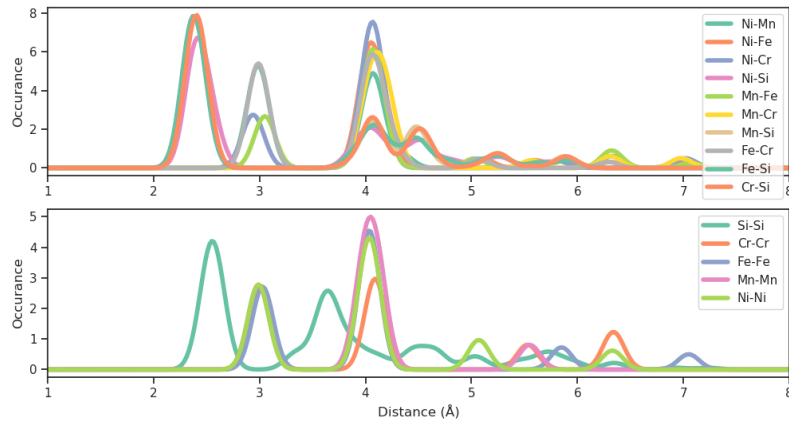
(b) B



(c) C



(a) D

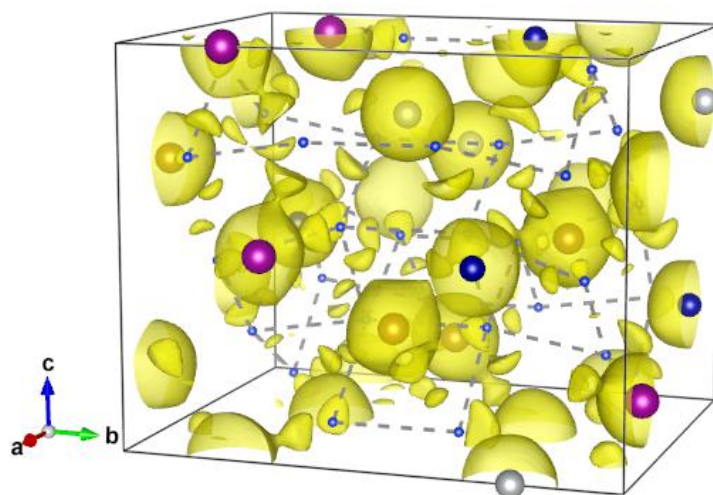


(b) E

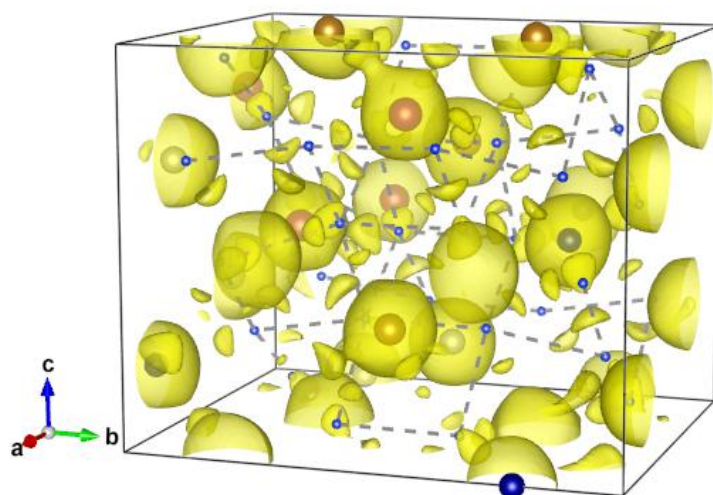
**Finish discussion pdfs, introduce CHGCAR**

**Discuss CHGCAR and summarize/conclude this section. Include aspects such as stability and magnetic configuration, important here to draw parallels and discuss the results in light of high-entropy alloys, SQS, DFT and thermoelectricity.**

**Transition into other methods and structures, present first results from SCAN and HSE06 for these 5 structures, discuss these results, but to lesser detail than PBE section. Then when finished with that, present, briefly discuss and summarize the results from all remaining structures, only include figures with good results, maybe others as well for the sake of comparison. The remaining data can be easily included in either the appendix or in a tabular format.**



(a) Structure B



(b) Structure D

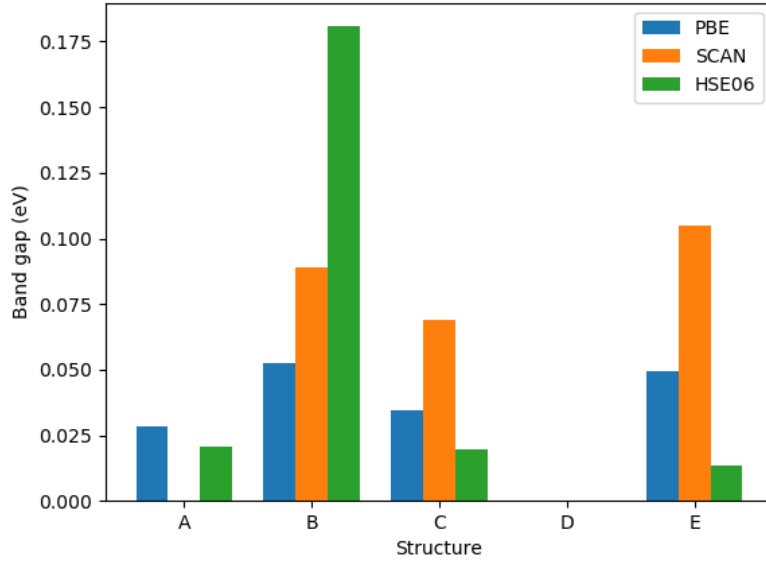


Figure 8.9: Band gap of CFMN (fesi2) all 5 SQSs with PBE, SCAN and HSE06

Looking at the results from different functionals, we observe that the hybrid functional HSE06 more or less agree with results of the PBE functional in terms of the actual presence of the band gap, while the size of the gap is up for debate. Especially in B, where we observe a band gap greater than 0.18 eV in comparison to 0.05 eV with PBE and 0.08 with SCAN. Below we show the total density of states around the fermi energy  $E_f$  for this structure with the HSE06 functional.

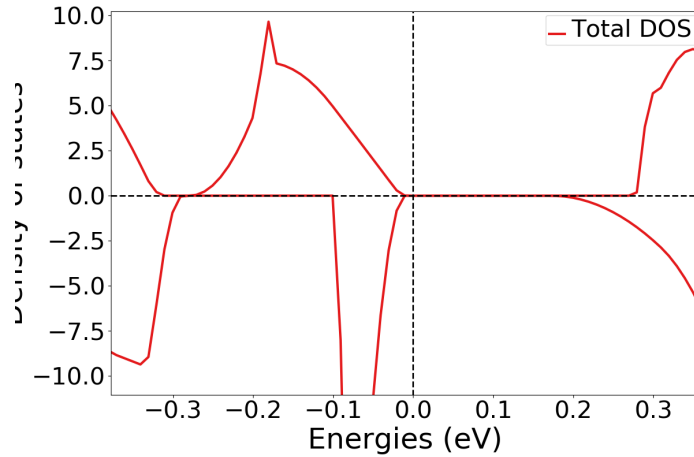


Figure 8.10: Density of states from HSE06 of  $FeSi_2$  CFMN structure B

If we now compare this to the density of states of structure E,

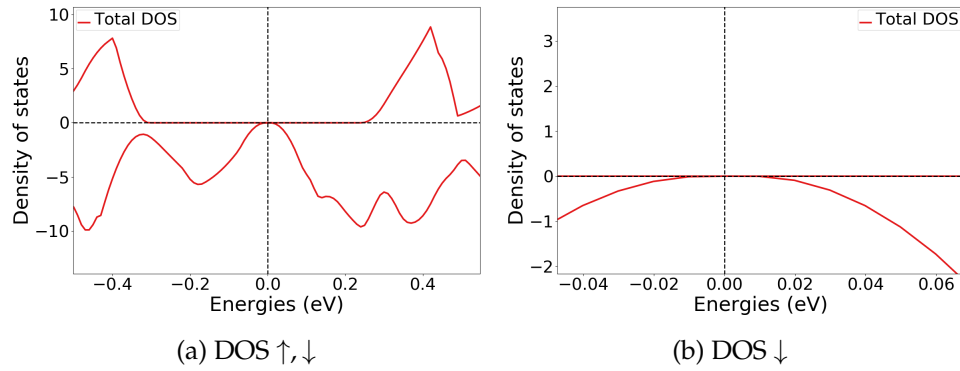


Figure 8.11: The density of states of CFMN ( $FeSi_2$ ) structure E for a) spin up and down, and b) focused on spin down

I think its relevant and interesting to in-depth analyze structure B, D, and E. B because of large band gap. D because no band gap, and E because this well represents the other structures A and C. One difference is the KS eigenvalues. Str D have both partial occupancy and nonphysical occupancy, ie above 1 and bellow zero both in PBE and HSE06. This is not the case for structures that exhibited band gaps. Here we have clear transition from 1 to 0. Without having done a broad investigation of all material. This seems to be the case in other compositions and cells and permutations as well. Where both partial occupants and nonphysical occupations result in metallic structures. Calculating the band gap with strict 1 and 0 conditions, lead to small band gaps in most structures. Furthermore, in structures of  $Fe_2Si$ , the difference in band where occupation transition from 1 to 0 between up and down, increases hugely compared to  $FeSi_2$  structures, talking close to 20 bands, opposed to maybe 2-5.

**Part IV**

**Conclusion**